

# Numerical and experimental study of dynamic elastomeric seals behaviour under actively controlled temperature conditions.

*M. Silvestri, E. Prati, A. Tasora*

*Dipartimento di Ingegneria Industriale, Università degli Studi di Parma, Italy*

## ABSTRACT

Clearance forming between rotating shafts and radial lip seals has been investigated both numerically and experimentally at various temperature conditions. Numerical models of clearance forming has been developed taking in account the effect of temperature, defining the material constituting properties according to empiric WLF function. Experiments have been performed with a special apparatus that allows control of lubricant temperature and level at each shaft speed . Results agree with simulations and give useful indications for practical applications.

## NOMENCLATURE

$\tau$	relaxation time	$p_d$	dynamic stress
$\Psi$	phase displacement	$p_s$	static stress
$\omega$	shaft speed	$p_t$	total stress
$R_a$	surface roughness	$t$	time
$T_g$	glass transition temperature	$x_d$	dynamic strain
$e_d$	dynamic eccentricity	$x_s$	static strain
$e_s$	static eccentricity	$x_t$	total strain

## 1. INTRODUCTION

Radial lip seals for rotating shafts are widely used to retain oil and exclude contaminants, often shielding bearings or journal boxes for rotating shafts. They are cheap, compact and can be used also in presence of vibrations or little radial runout.

Many types of seals are available, differing in material and geometry in order to be suitable for several operating conditions. In spite of this variety, they are always built up by three fundamental elements: an elastomeric ring, a metallic stiffening insert and a garter spring (see figure 1).

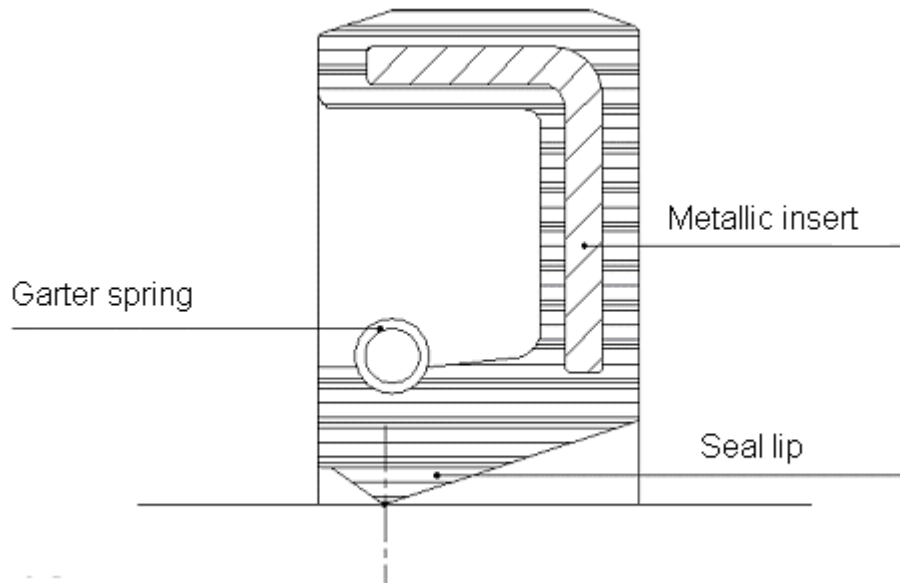


**Figure 1: Section of radial lip seal.**

The ring ends, at shaft interface, with a lip; the garter spring stiffens the lip and assures a better uniformity of the bearing pressure between seal and shaft on varying working conditions. Rotary lip seals are very simple mechanical system components that have highly sophisticated and complex operating mechanisms. Investigations on the sealing and lubrication of radial lip seals have a long tradition (1), (2), (3), involving different disciplines including hydrodynamics, materials science and tribology. Their behaviour has been explained with the influence of temperature (4) and visco-elastohydrodynamic lubrication (5), (6), (7), but such explanations do not completely justify experimental results that show several stages of the leakage rate at different shaft rotating speed (8) (9) (10).

Preceding works have shown many experimental results achieved both in working conditions and with simulation apparatus by means of several transducers: cameras, torque meters, accelerometers (for *Frequency Response Function analysis*), thermocouples, flowmeter and, recently, a strain gauge transducer mounted on a machine that simulates actual operating conditions (10), (11).

Available experimental data also made possible to start implementing a numerical simulation of the phenomenon with Finite Elements Method. In (11) is described a first approach where dynamic seals behaviour was approximated by a non-linear Mooney-Rivlin model. This method was probed to be suitable for high frequencies rotating stress and improved in (12). In order to reach a better synthesis of the tests results and the theoretical studies, we proceeded with experimental and numerical tests aimed at simulating temperature effects in various working conditions.

## **2. NUMERICAL ANALYSIS**

In (10) and (11) has been described a FEM seal model obtained as solid of rotation from a simplified section and its reliability has been validated by comparisons of experimental results of Frequency Response Function analysis. A further development (12) took account of temperature effects on material constitutive law and has been resumed in this paper.

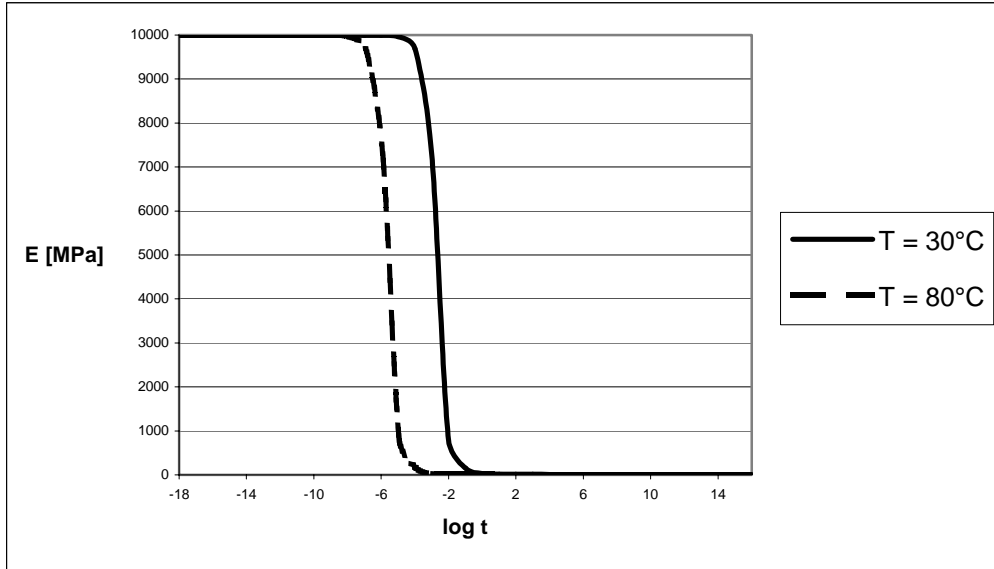


**Figure 2: Relaxation curve shift.**

The approach is based on repeating the simulation at various elastomer temperature, so *Prony series*, that describes material constituting properties, changes according to empiric *Williams - Landell - Ferry* shift function, that gives the glass transition frequency shift. When stress frequency reaches the transition zone, the seal lip cannot follow shaft movement and clearance happens.

In detail, simulations exploit the ability of ABAQUS software to simulate varying boundary conditions applying to the seal lip a static strain  $x_s$  and a sinusoidal one,  $x_d(t)$ , obtaining altogether:

$$x_t(t) = x_s + x_d(t) = x_s + |x_d| \cos \omega t$$

The corresponding total stress results are:

$$p_t(t, y) = p_s(y) + p_d(t, y) = p_s(y) + |p_d(y)| \cos(\omega t + \Psi)$$

So is possible to suppose that the detachment happens if, in  $i^{\text{th}}$  node, where the stress is maximum, dynamic stress become greater than the static one, giving:

$$p_t(t, y_i) < 0$$

Physically this happen near to the glass transition of the elastomer, that cause a quick increase in rubber stiffness. Table 1 shows the *Prony series* coefficients used at reference temperature of 303 K, while the glass transition temperature has been estimated as  $T_g = 253$  K. Curves in figure 2 exemplify as a relaxation curves shifts passing from reference temperature to working temperature (353 K).

The geometric modeling has been made up both with a simplified 2D model (see figure 3) and with a 3D model (see figure 4). The first has been useful to quickly adjusting conditions and to verify results comparing with (5), while the 3D model is more realistic and takes in account also the tangential stress that the shaft generates on the contact surface.

**Table 1: Prony series coefficients**

$g_1 = 0,9504$	$\tau_1 = 0,003$ [s]
$g_2 = 0,045$	$\tau_2 = 0,072$ [s]
$g_3 = 0,003$	$\tau_3 = 1,01$ [s]
$g_4 = 0,0003$	$\tau_4 = 19,9$ [s]
$g_5 = 0,00013$	$\tau_5 = 367$ [s]
$g_6 = 0,00011975$	$\tau_6 = 3606$ [s]
$g_7 = 0,0000828$	$\tau_7 = 47347$ [s]

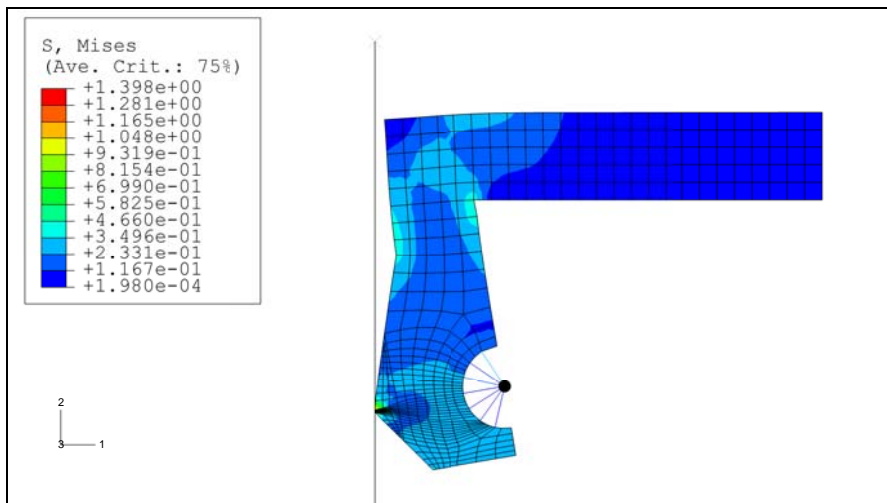


**Figure 3: Von Mises stress in bidimensional model.**

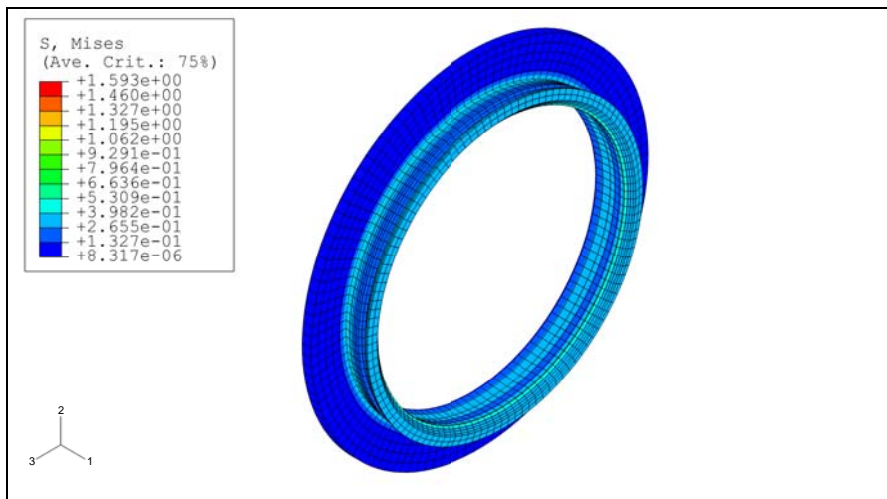


**Figure 4: Von Mises stress in tridimensional model**

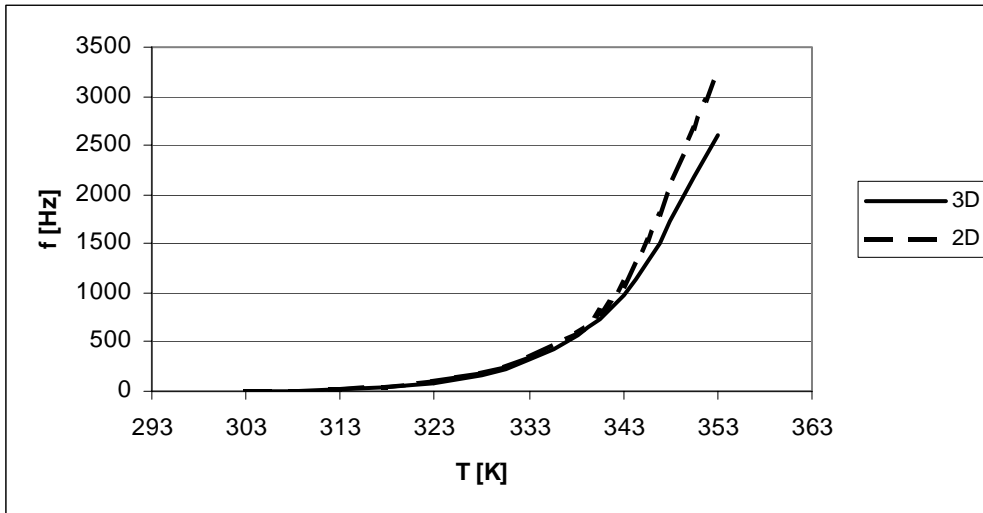


**Figure 5: Comparison of clearance frequencies in 2D and 3D models.**

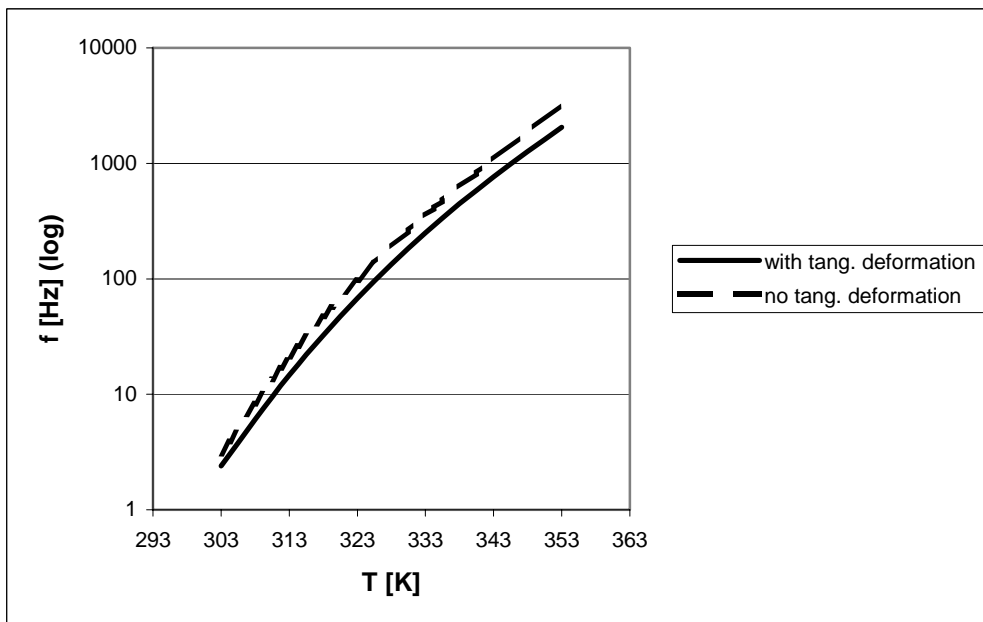


**Figure 6: Effect of tangential stress**

Bidimensional and tridimensional models agree on clearance frequencies, as curves in figure 5 show. Figure 6 highlights the contribution of tangential stress to reaching the clearance forming.

### 3. TEST RIG

The test rig is made up of three subsystems: a rotating shaft machine that allows a repeat of actual working conditions, an oil circuit that controls the temperature and the level of the fluid and several measuring and data acquisition instruments devoted to observe the presence of clearances between the shaft surface and the seal lip.

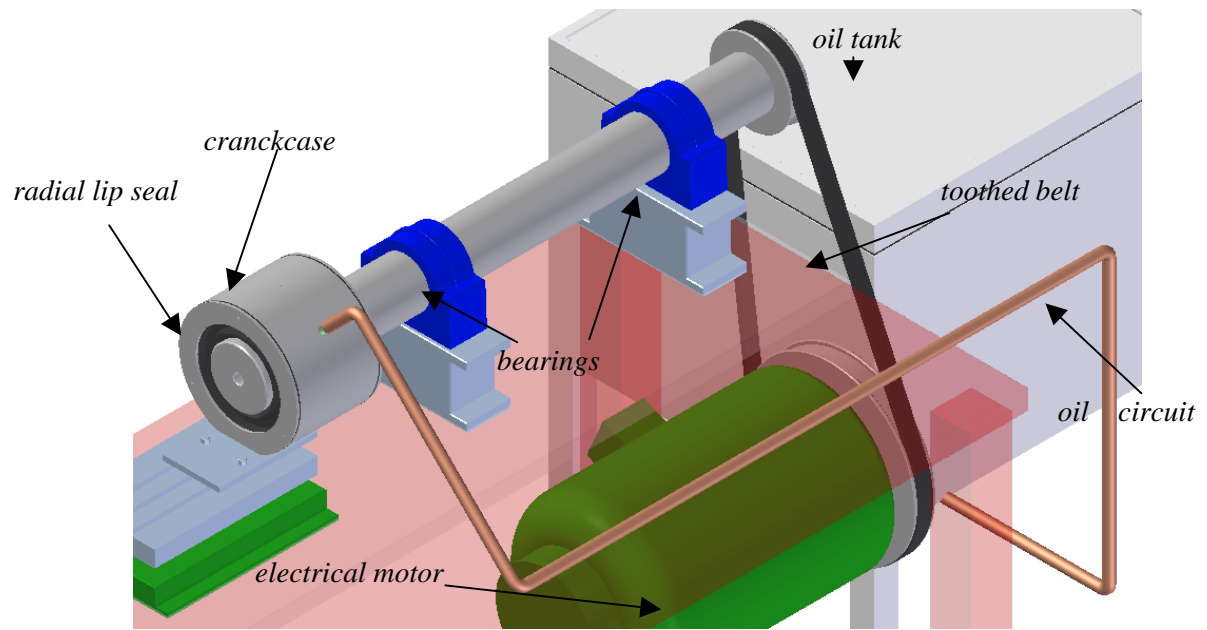


**Figure 7: The test machine**

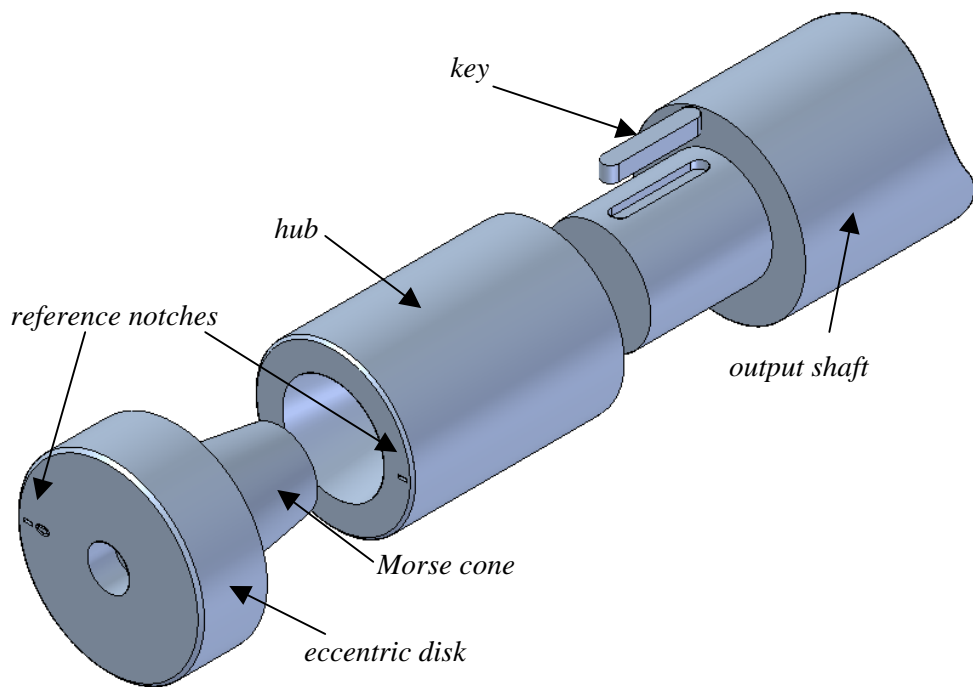


**Figure 8: The end of the output shaft**

**3.1 The machine**

The mechanism is mainly constituted by a direct current electrical motor moving a shaft through a toothed belt transmission (see figure 7). The speed is manually controlled and can vary continuously in the 300-8000 rpm range (at the output shaft). At the end, the shaft has a disk of circular profile which is in contact with the test seal. The dynamic eccentricity of this disk can be set to any value between 0 and 0.52 mm by mean of a conical coupling (see figure 8). The disk is polished and has a surface roughness  $R_a = 0.188 \mu\text{m}$ , as measured by using a profilometer. The position of the fixed seal housing can also be adjusted, giving the desired static eccentricity.

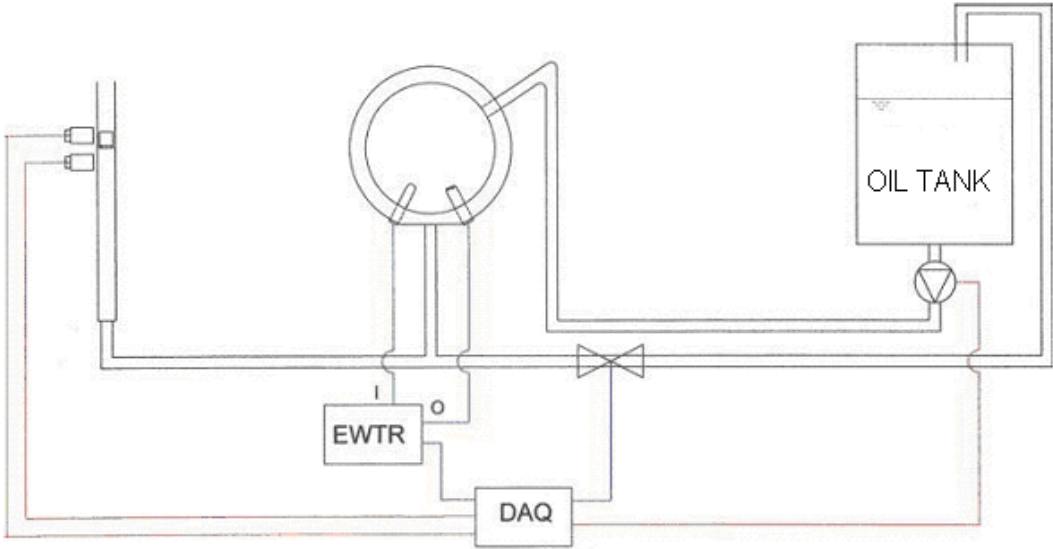


**Figure 9: The lubricant circuit**

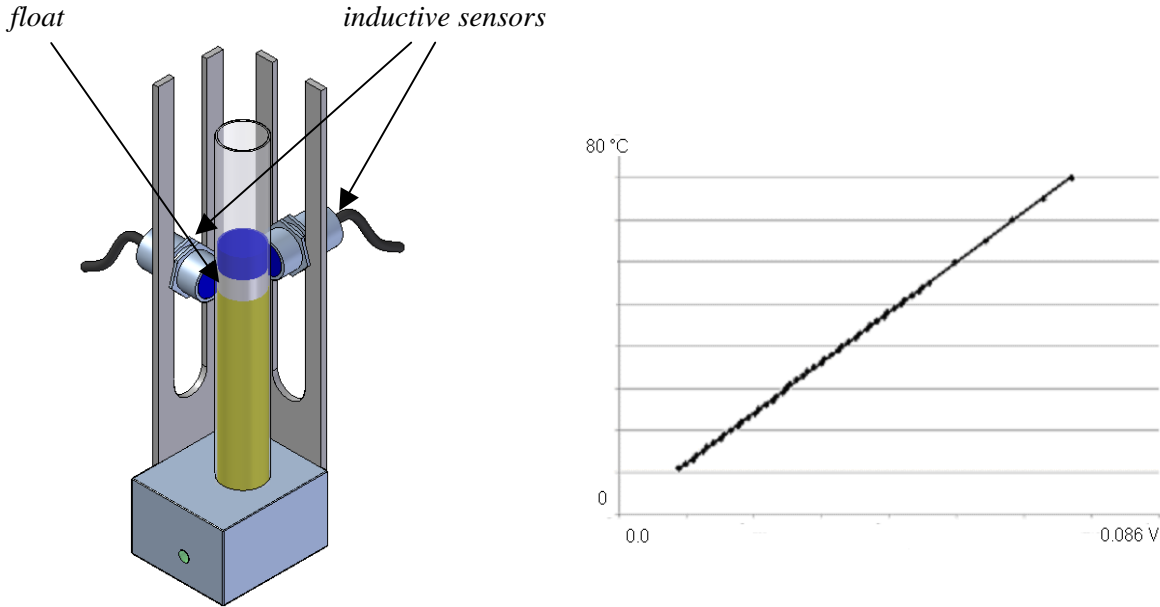


**Figure 10: Level sensor and temperature sensor calibration curve.**

### 3.2 The lubricant circuit

This circuit (see figure 9) allows control of both the temperature and the level of the lubricant in the crankcase; as shown in figure 9, it is made up by an oil cooler, a gear pump, a crankcase heater, temperature and level sensors. These devices and solenoid valves are driven by the same I/O board that is used for data acquiring, so the control software has been written in LabView environment.

In order to ensure stability and robustness in the control loop, the most critical aspect is given by the relative low outflow of the oil, particularly at low temperatures. Since, of course, the crankcase cannot be pressurized (regarding this matter, the top of the box has been drilled), the fluid must flow only by gravity with very little head, so the limited discharge of warm oil could prevent heat disposal at high speed. The adopted solution consists in mounting an adjustable-with-by-pass flow control valve on pump delivery, partially starting to change the oil in the box on increasing shaft speed, so that the thermic transient remains sufficiently slow in every running condition. In particular, it is possible to obtain steady state lubricant running temperature in the 30-70 °C range with the accuracy of  $\pm 1$  °C.

On the other side, adjusting the lubricant level is necessary for controlling the partially flooded conditions of the contact between the seal and the shaft surface. Seeing that inside the case there is not enough room for sophisticated level sensors, a communicating glass pipe with a float, shown in figure 10, has been adopted to obtain a reliable indicator that can be detected by cheap inductive sensors. The sensor position is easily adjustable tightening them on vertical brackets and so it is possible to set both the maximum and the minimum fluid level with the test rig working.

Oil temperature is measured by a Pt-100 resistor mounted inside the crankcase. Its calibration curve (see figure 10) shows an almost linear behaviour along the whole working range.

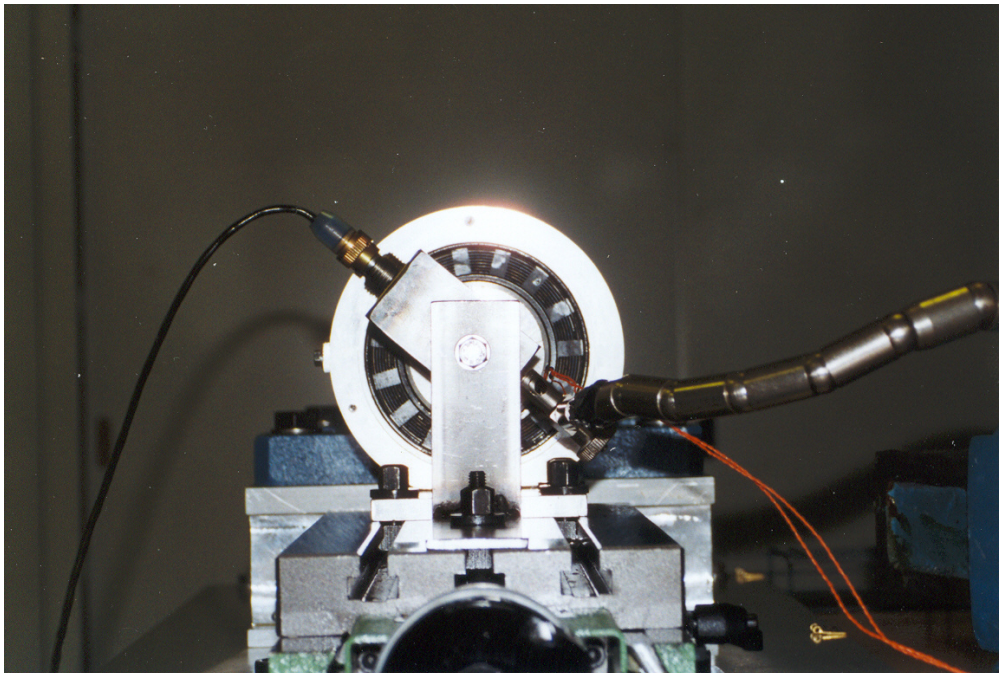
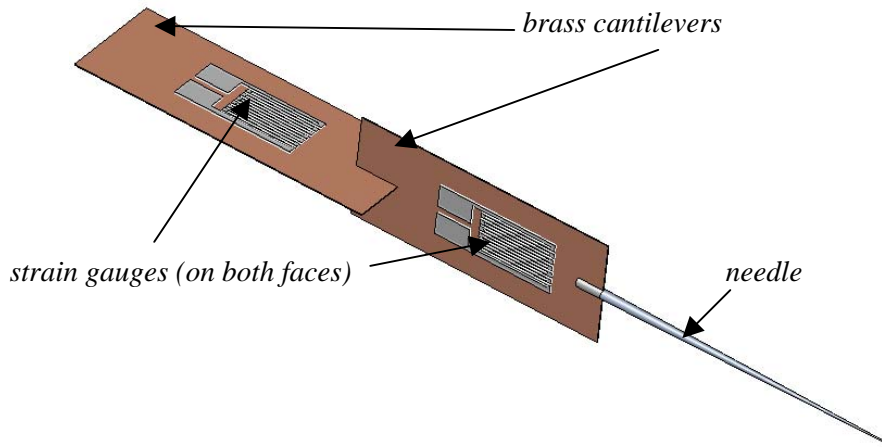
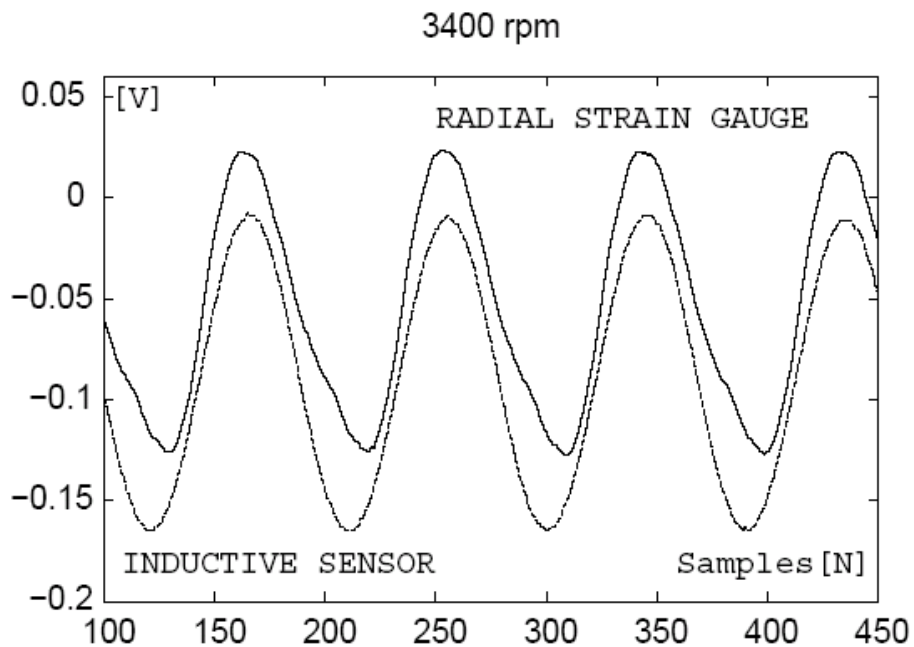


Figure 11: Sensors mounting





**Figure 12: Strain gauge transducer**



**Figure 13: Lip and shaft profile radial displacement**

### 3.3 Measuring Instruments

As figure 11 shows, an inductive sensor collects the surface of the disk profile with which the seal is coupled and hence the radial displacement imposed on the lip. This signal is useful to be compared with the lip position, detected by a strain gauge transducer (see figure 12): when the two signals separate each other (see figure 13) there is a clearance between the lip and the disk.

In details, the transducer is made up by two brass cantilever located at right angles to each other, of dimensions  $25 \times 12$  mm. On each cantilever are glued two strain gauges, one for each side. At the end of the brass plate there is a steel needle with diameter 0.5 mm.

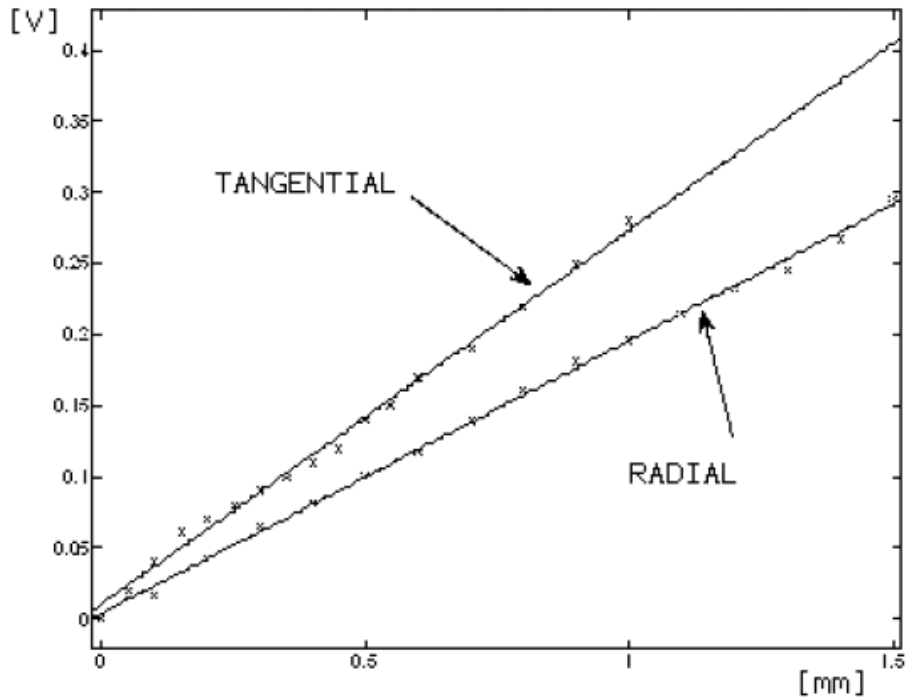


**Figure 14: Transducer calibration curves**

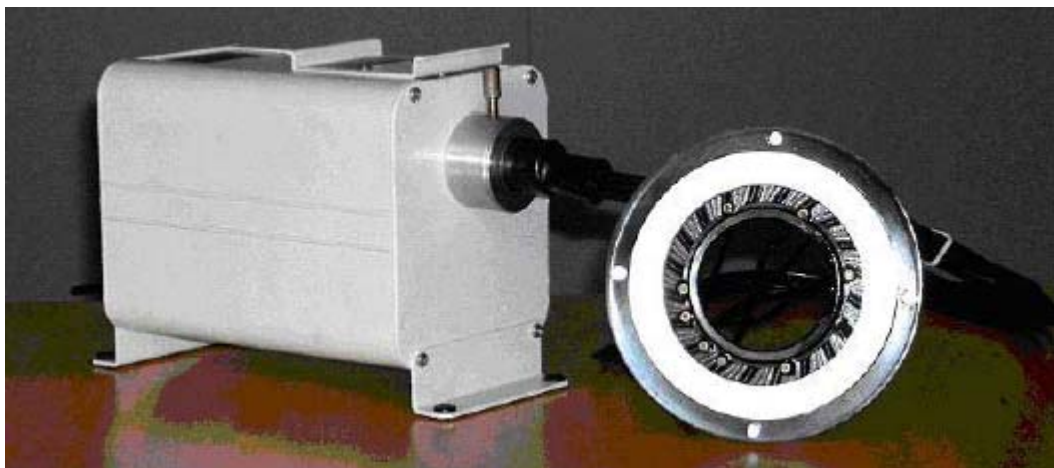


**Figure 15: Fiber optic mounted on the back lid**

One can note that the inductive sensor and the cantilevers transducer are mounted with a phase difference of  $180^\circ$ , as the two signals may easily superimposed (inverting one of them). The transducer depicted in figure 12 is inserted in the lip, in the zone corresponding to the maximum eccentricity.

The apparatus also includes a signal conditioning amplifier Instrument Division 2120A for the strain gauges, a Kaman measuring systems P3500 for the inductive sensor and a National Instruments PCI-MIO- 16E board that collects both the signals.

Calibration curves of both radial and tangential signals are shown in figure 14. They have been calculated interpolating measurements obtained in 25 equally spaced points in the range of needle tip displacement of  $0 \div 1.5$  mm. Graphs highlight a good linearity in transducer response. A fiber optic lamp (see figure 15) lights the seal from the inside the housing, allowing direct verification, when the measurements point out a clearance, the presence of a gap between the lip and the disk.

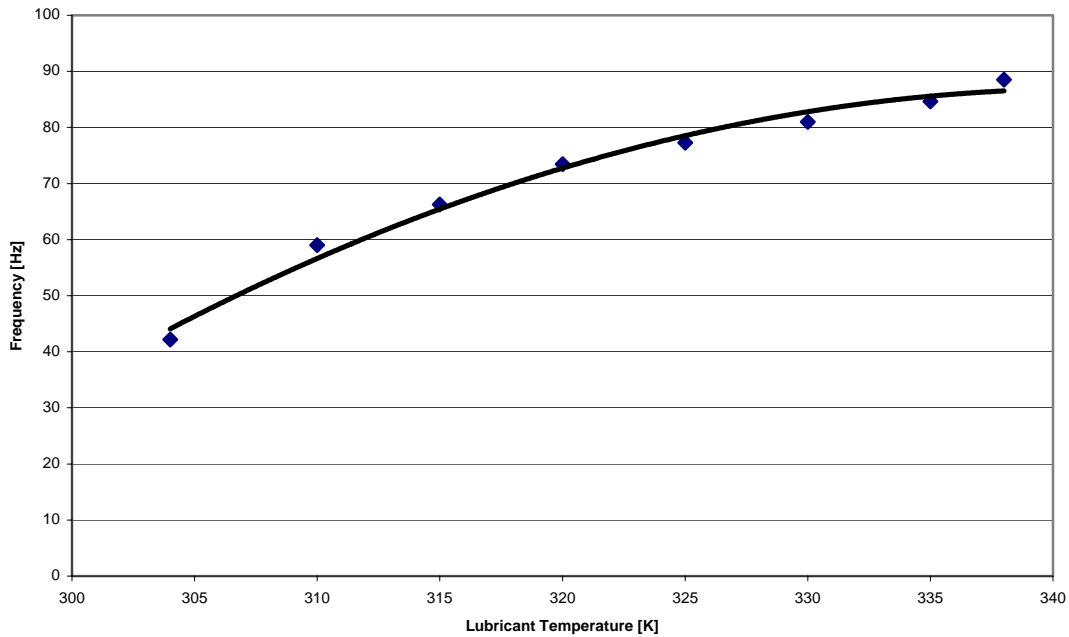


**Figure 16: Clearance forming frequency (test measurements,  $e_d=0,4$  mm)**

#### 4. RESULTS

The strain gauge transducer allows robust recognition of the presence of clearances between seal lip and shaft, in particular studying the derivative of a function obtained as Fourier series approximation of the acquired signal (12).

It is known (8), (9) that working cycles have a great influence on the seal behaviour. In order to reach seal steady state, five working cycle of one hour at 1000 rpm have been done. Then, data have been collected varying the fluid temperature between 31 and 65 °C with steps of 5 °C and the shaft speed between 500 and 6000 rpm with steps of 100 rpm. Sampling rate vary from 1000 to 6000 Hz. The graph in figure 16 shows the clearance forming frequency observed at various lubricant temperatures. As may be expected, at higher temperature the lip become more able to follow the shaft movement and the clearance occurs at higher frequencies.

Figure 17 shows the simulation results at various dynamic eccentricity values. The meaning of these graphs can be correctly understood referring to hypotheses on which the simulation is based. In particular, the absence of lubricant causes the detachment of the lip at low frequencies, as experimentally proved in (13). Not surprisingly, the comparison with the experimental curve highlights that the pressure in the oil film between seal and shaft greatly improves the sealing effect. Nevertheless, once this difference is taken into account, both graphs show frequency increment at increasing temperatures. Underestimating clearance frequency at low temperatures also causes quite a different shape in the graph trends: while the experimental curve can be approximated by a parabolic curve with decreasing slope, the FEM analysis result follows a 4<sup>th</sup> degree polynomial with increasing slope.

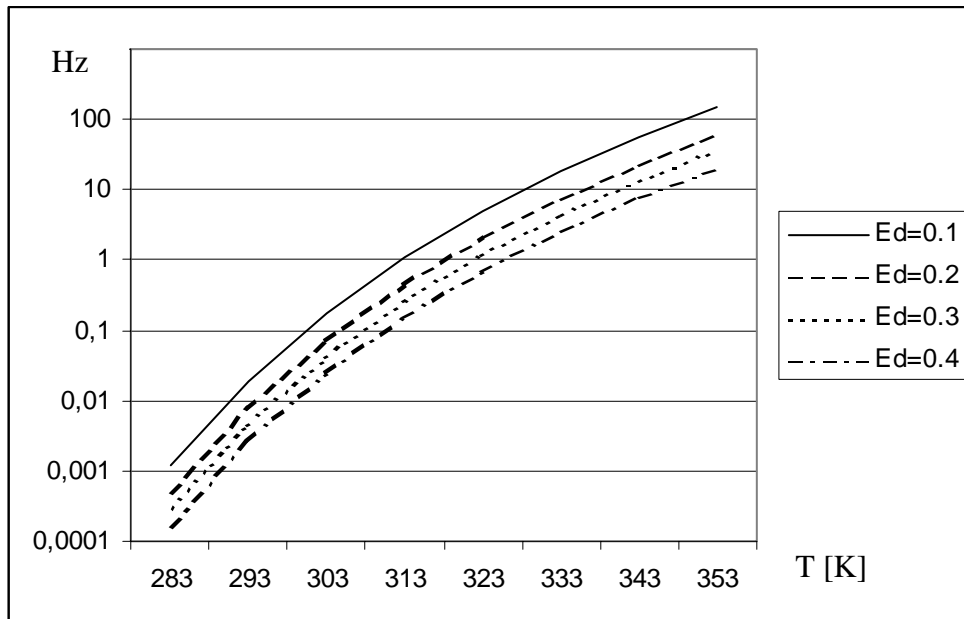


**Figure 17: Clearance forming frequencies (FEM simulations)**

## 5. CONCLUSIONS

Clearance forming between rotating shafts and radial lip seals has been investigated both numerically and experimentally at various temperature conditions. In both cases there is a significant influence of the temperature on the clearance forming frequency.

Further studies will include measuring simultaneously the clearance area and the leakage rate, with the aim of evaluating if, on varying temperature, it is predominantly influenced by the clearance size or by the lubricant viscosity.

Results suggest that low temperatures in working machines (e.g. during a transient) should be carefully considered in order to avoid unwanted lubricant leakage, particularly in the presence of large eccentricities.

## ACKNOWLEDGEMENTS

This research was supported by the grant of the Università degli Studi di Parma. The authors acknowledge the useful help of Ing. Alberto Mazzoni and Ing. Mattia Cenci in test activities.

## REFERENCES

- (1) Jagger E. T., *Study of the Lubrication of Synthetic Rubber Rotary Shaft Seals*, Proceedings of the Conference on Lubrication and Wear, I.Mech.E., pp. 409-415, 1957.
- (2) Müller, H.K., *Concepts of sealing Mechanism of Rubber Lip Type Rotary Shaft Seals*, Proceedings of the 11th International Conference on Fluid Sealing, B.H.R.A., Paper K1, pp. 698-709, 1987.

- (3) Salant, R.F., *Numerical Analysis of the Flow Field Within Lip Seals Containing Microundulations*, ASME Journal of Tribology, Vol. 114, pp. 485-492, 1992.
- (4) Stakenborg, M.J.L., *On the Sealing Mechanism of Radial Lip Seals*, Tribology International, Vol. 21, pp. 335-340, 1988.
- (5) Stakenborg, M.J.L., van Leeuwen, H.J. and ten Hagen E.A.M., *Visco-Elastohydrodynamic (VEHD) Lubrication in Radial Lip Seals: Part I - Steady-State Dynamic Viscoelastic Seal Behavior*, ASME Journal of Tribology, Vol. 112, pp. 578-583, 1990.
- (6) van Leeuwen, H.J., and Stakenborg M.J.L., *Visco-Elastohydrodynamic (VEHD) Lubrication in Radial Lip Seals: Part 2 - Fluid Film Formation*, ASME Journal of Tribology, Vol. 112, pp. 584-592, 1990.
- (7) G. Colombo ed E. Prati, *Condizioni di Tenuta con Guarnizioni Radiali per Alberi Rotanti*, Atti del XV Congresso AIMETA di Meccanica Teorica e Applicata, 26-28 Settembre, Taormina, Italy, Sommario pag. SP ME 20, 2001.
- (8) M. Amabili, G. Colombo and E. Prati, *Leakage of Radial Lip Seals at Large Dynamic Eccentricities*, Proceedings of the 16th International Conference on Fluid Sealing, September 18-20, Brugge, Belgium, pp. 321-333, 2000.
- (9) M. Amabili, G. Colombo and E. Prati, *On the Leakage of Radial Lip Seals*, Proceedings of 2000 AIMETA International Tribology Conference, 20-22 September, L'Aquila, Italy, pp. 565- 572, 2000.
- (10) M. Silvestri, E. Prati, A. Tasora, *Un modello del comportamento di tenute dinamiche al variare della temperatura*, Atti del XVI Congresso AIMETA di Meccanica Teorica e Applicata, Ferrara, Italy, 9-12 settembre, su CDROM, 2003.
- (11) M. Silvestri, E. Prati, A. Tasora, *Dynamic Seals Behaviour under Effect of Radial Vibration*, Proceedings of 14th International Colloquium Tribology, Tribology Lubrication Engineering, January 13-15, Stuttgart, Germany, 2004, pp. 1247-1254, 2004.
- (12) M. Silvestri, E. Prati, A. Tasora, *Numerical Analysis of Sealing Conditions in Elastomeric Rings*, Proceedings of IV AITC, Rome, Italy, September 14-17 pp. 509-606, 2004.
- (13) E. Prati, *Dynamic Behaviour of Radial Lip Seals Under Effect of Shaft Eccentricity*, Proceedings of the 10<sup>th</sup> International Conference on Fluid Sealing, Innsbruck, Austria, April 3-5 pp.123-138, 1984.